The Role of Baseband Noise and Its Upconversion in HBT Oscillator Phase Noise

Marcel N. Tutt, Dimitris Pavlidis, *Fellow, IEEE,* Ali Khatibzadeh, and Burhan Bayraktaroglu, *Senior Member, IEEE*

Abstract— **The phase noise spectral density ($\pounds(f_m)$) of an 11.02–GHz heterojunction bipolar transistor (HBT) dielectric resonator oscillator (DRO) has been investigated in terms of the HBT's low frequency noise and the oscillator's upconversion coefficient. Experimental studies have been used for this purpose and the measured $\pounds(f_m)$ ranged from −89 dBc/Hz to −101 dBc/Hz at a 10–kHz offset frequency (best phase noise spectral density performance was −124 dBc/Hz at 100 kHz). It was shown that, in most test cases, $\pounds(f_m)$ can be described by the upconversion of the HBT's baseband noise. As a result the frequency dependence, of $\pounds(f_m)$, is dictated by the low frequency noise spectrum rather than the upconversion itself. Deviation from pure $1/f$ frequency dependence found for the HBT's baseband noise at frequencies above 100 Hz resulted in $d\pounds(f_m)/d(f_m)$ deviating from about −30–dB/decade rate. Reduced oscillator phase noise at high collector current is attributed to reduced upconversion in the oscillator.**

I. Introduction

HETEROJUNCTION bipolar transistors (HBT's) have shown excellent performance in microwave circuits [1]–[4]. Their power capability makes them very attractive for power amplifiers and oscillators. Today, microwave and millimeterwave oscillator applications are addressed by GaAs MESFET and Silicon (Si) bipolar junction transistors (BJT's). One of the most important characteristics of an oscillator is its spectral purity. A common measure of spectral purity is the ratio of the noise power in a 1-Hz bandwidth in one noise sideband at an offset frequency, f_m, from the carrier to the power of the carrier. This measure is called the noise power spectral density and it is represented by $\pounds(f_m)$ with units of dBC/Hz. It is generally accepted that Si BJT's display the best phase noise performance (lowest $\pounds(f_m)$) of all transistor based oscillator's.

YIG tuned oscillators, using Si BJT's, have demonstrated useful operation up to 18 GHz [5] with $\pounds$ (20 kHz) measured to be between −100 and −105 dBC/Hz over the entire tuning range of 2–18 GHz. Si BJT's and GaAs MESFET's were compared directly, at 6 GHz, in [6]. The Si BJT DRO had $\pounds(f_m) \approx$ −75 and −100 dBc/Hz at 1 and 10-kHz offset frequencies, respectively. The MESFET DRO had $\pounds(f_m) \approx -67$ and −95 dBC/Hz at the same offset frequencies. The same holds true in the commercial arena where for example, GaAs MESFET and Si BJT based DRO's typically provide $\pounds$ (10 kHz) ≈ −90 and −95 dBC/Hz, respectively [7]. FET based oscillators are capable of operating at much higher oscillating frequencies. A MMIC HEMT oscillator has been realized at 130 GHz through the use of an InP based material system instead of a GaAs based system [8]. Dielectric resonator stabilized MESFET oscillators in work by [9]–[11] demonstrated that MESFET based oscillators could also provide excellent $\pounds(f_m)$ characteristics.

HBT based oscillator circuits have been built using free-running, VCO, and DRO approaches [2], [4], [13]–[17]. Using a free-running design at 37.7 GHz, $\pounds$(100 kHz)= −82 dBC/Hz was obtained by [2]. In [4] a DRO operating at 11.06 GHz achieved $\pounds(f_m) = -76$ and −102 dBC/Hz at 1 and 10 kHz, respectively. All of the $\pounds(f_m)$ listed above can be approximately compared with scaling. Using the relation of Leeson [18], $\pounds(f_m)$ scales with operating frequency by ω_0^2. Scaling with respect to offset frequency is a little more difficult. For the case where upconversion of ideal $1/f$ noise dominates, within the resonator bandwidth, $\pounds(f_m)$ varies as $1/f_m^3$.

HBT based oscillators are expected to provide better $\pounds(f_m)$ performance than FET based circuits due to reduced low frequency noise. The best low frequency noise results have been obtained by Hayama et al [14] who reported $1/f$ noise corner frequencies of 400 Hz. In order for HBT oscillators to achieve their ultimate performance, a systematic study of the factors which impact the oscillator noise is required. Considerable effort has been expended on the study of MESFET based oscillators [11], [12], [19]–[21] are examples. On the otherhand, HBT based oscillators are relatively new and to date a systematic study of the parameters which contribute to their characteristics has not been carried out. This paper presents the results of the first systematic experimental study of the role of the device baseband noise ($1/f$ noise), the upconversion coefficient (K'_{FM}), and the low frequency base termination in the phase noise spectral density of HBT oscillators. The baseband noise is an inherent device property which, through upconversion, can degrade the spectral purity of the oscillator. On the otherhand, K'_{FM} is a characteristic of the oscillator circuit and the active device which indicates how sensitive the oscillator is to phase modulation by an external signal. The results of this work show the significance

Manuscript received April 13, 1994; revised March 29, 1995. This work was supported by Contract MDA904-90-C-4096, ARO (Contract DAAL03-92-G-0109), and NASA (Contract NAGW-1334).

D. Pavlidis is with the Solid-State Electronics Laboratory, Department of Electrical Engineering and Computer Science, University of Michigan, Ann Arbor, MI 48109-2122 USA.

M. Tutt was with the University of Michigan, Ann Arbor, he is now with the Corporate Research and Development Laboratory, Texas Instruments, Dallas, TX 75265 USA.

A. Khatibzadeh is with Central Research Laboratories, Texas Instruments, Dallas, TX 75265 USA.

B. Bayraktarogl is with Westinghouse Electronics Systems Group, P.O. Box 1521, Baltimore, MD 21203 USA.

IEEE Log Number 9412052.

of the upconversion of the HBT's baseband noise. Section II presents the theoretical basis and experimental procedure for this work. Starting from a general phase noise relationship, a simplified relation is obtained for the phase noise in terms of just K'_{FM}, and the oscillator baseband noise. Section III describes both the HBT and the oscillator studied in this work. Results of phase noise spectral density and single sideband amplitude modulation (SSB-AM) noise measurements as a function of bias, and low frequency base termination are presented in Section IV. The measured K'_{FM} of the oscillator used here is compared with the experimental results for other oscillators in Section V. Section VI describes the baseband noise characteristics of the HBT used in the oscillator. The measured $\pounds(f_m)$ is compared with that calculated using the measured K'_{FM} and device baseband noise in Section VII. Finally, conclusions are presented.

II. Noise Upconversion

A. Theory of Noise Upconversion

In the early work by Leeson [18], $\pounds(f_m)$ was expressed heuristically using physical arguements. In this section, the $\pounds(f_m)$ is expressed in terms of: 1) the upconversion coefficient, K'_{FM}, and 2) the HBT's baseband noise. The analysis, of the oscillator noise, is based on the approach used by Riddle [23]. This approach is used since it provides a means for expressing the $\pounds(f_m)$ in terms of circuit and device parameters which is not done using Leeson's approach. It is based on the idea that the oscillator can be represented by a feedback network with additive noise at the input and the oscillator signal is the output

$$(n_i + jn_q)e^{j\omega_0 t} = D(A,\omega,\epsilon)(A_0 + m + j\beta)e^{j\omega_0 t} \tag{1}$$

n_i and n_q are the in-phase and quadrature components of the additive noise. D is the inverted transfer function consisting of a real part, U, and an imaginary part, V. A_0 is the mean value of the oscillator amplitude. ω_0 is the mean value of the oscillator frequency, ω. ϵ represents the bias condition of the active device of the oscillator. m and β are the amplitude and phase modulation, respectively. For the noise analysis D is expanded in a Taylor Series (only the first order terms are retained) and (1) can be written as two equations

$$\begin{aligned} n_i = &\left[U_0 + A_0\frac{\partial U}{\partial A} + j\Delta\omega\frac{\partial V}{\partial \omega}\right]m \\ &+ \left[j\Delta\omega\frac{\partial U}{\partial \omega}\right]\beta + A_0\Delta\epsilon\frac{\partial U}{\partial \epsilon} \end{aligned} \tag{2}$$

$$\begin{aligned} n_q = &\left[A_0\frac{\partial V}{\partial A} - j\Delta\omega\frac{\partial U}{\partial \omega}\right]m \\ &+ \left[U_0 + j\Delta\omega\frac{\partial V}{\partial \omega}\right]\beta + A_0\Delta\epsilon\frac{\partial V}{\partial \epsilon}. \end{aligned} \tag{3}$$

U_o is a constant term arising from the expansion of D. $\Delta\epsilon$ represents the perturbation of the bias which can arise due to bias supply fluctuations or device baseband noise. In this work only baseband noise is considered.

These equations can be put into a convenient matrix equation form

$$\begin{bmatrix} \frac{n_i}{A_0} - \Delta\epsilon\frac{\partial U}{\partial \epsilon} \\ \frac{n_q}{A_0} - \Delta\epsilon\frac{\partial V}{\partial \epsilon} \end{bmatrix} = \begin{bmatrix} M_{11} & M_{12} \\ M_{21} & M_{22} \end{bmatrix} \begin{bmatrix} m \\ \beta \end{bmatrix}. \tag{4}$$

The M_{ij} terms are the modulation transfer terms. M_{11} is the amplitude to amplitude conversion, while M_{22} is the phase to phase conversion. The off-diagonal terms are cross-conversion terms. M_{21} is the amplitude to phase conversion, while M_{12} is phase to amplitude conversion. The significance of cross-conversion is affected directly by the oscillator design. It will be minimized when the oscillator stability is maximized.

The oscillator phase and amplitude noise spectral densities, $S_\phi(\omega_m)$ and $S_A(\omega_m)$, respectively, are given by

$$S_\phi(\omega_m) = \overline{\beta^2} \tag{5}$$

$$S_A(\omega_m) = \overline{m^2} \tag{6}$$

where $\omega_m = \Delta\omega$ is the frequency offset from the carrier.

Several points are demonstrated by these equations: 1) baseband noise contributes to the AM and PM noise; 2) additive noise at the oscillation frequency also contributes directly to the AM and PM noise and 3) AM noise can be converted to PM noise and vice versa. In this work, we are investigating the role of the upconversion of the HBT's baseband noise in the oscillator's PM noise.

In the case where the cross-conversion terms are zero, $S_\phi(\omega_m)$ is given by

$$S_\phi(\omega_m) = \frac{\overline{\left(\frac{n_q}{A_0}\right)^2}}{\left(\omega_m\frac{\partial V}{\partial \omega}\right)^2} + \frac{\overline{\Delta\epsilon^2}\left|\frac{\partial V}{\partial \epsilon}\right|^2}{\left(\omega_m\frac{\partial V}{\partial \omega}\right)^2} \ (\mathrm{Hz^2/Hz}) \tag{7}$$

where we have made use of the fact that $U_0 \ll \omega_m\frac{\partial V}{\partial \omega}$ [23]. The first term contributes a $1/f^2$ component due to the ω_m^2 term. The second term accounts for the upconversion of the baseband noise ($\overline{\Delta\epsilon^2(\omega_m)}$) and has a $1/f^3$ dependence if $\overline{\Delta\epsilon^2(\omega_m)}$ has a $1/f$ dependence. Since the low frequency noise will have a $1/f^\alpha$ dependence, it will be more significant than the additive noise component in our measurement range. As a result, we will assume that the second term will be dominant. Therefore, we can write

$$S_\phi(f_m) \approx \frac{\overline{\Delta\epsilon^2(\omega_m)}}{\omega_m^2\tau_g^2}\left|\frac{\partial V}{\partial \epsilon}\right|^2 \tag{8}$$

where we have used$\tau_g = \left|\frac{\partial V}{\partial \omega}\right|$ [24]. For low level modulation, $\pounds(f_m)$ is approximated by

$$\pounds(f_m) \approx \frac{S_\phi(f_m)}{2} = \frac{\overline{\Delta\epsilon^2(f_m)}}{2\omega_m^2\tau_g^2}\left|\frac{\partial V}{\partial \epsilon}\right|^2. \tag{9}$$

The upconversion coefficient, K'_{FM}, is defined as

$$K'_{\mathrm{FM}} = \left|\frac{\partial V}{\partial \epsilon}\right|\frac{1}{2\pi\tau_g} \ (\mathrm{MHz/V}). \tag{10}$$

So $\pounds(f_m)$ is given by

$$\pounds(f_m) \approx \frac{\overline{\Delta\epsilon^2(f_m)}}{2f_m^2}K'^2_{\mathrm{FM}}. \tag{11}$$

$\frac{K'_{\rm FM}}{\Delta\epsilon^2(f_m)}$ quantifies how strongly the low frequency noise, $\Delta\epsilon^2(f_m)$, is upconverted. It is a function of both the oscillator circuit and the HBT (through τ_g and $\left|\frac{\partial V}{\partial \epsilon}\right|$). For the case where f_m is sufficiently small, $K'_{\rm FM}$ can be expressed in terms of the oscillator $\tau_g = \frac{2Q}{\omega_0}$ [23]

$$K'_{\rm FM} = \left|\frac{\partial V}{\partial \epsilon}\right| \frac{\omega_0}{4\pi Q}. \tag{12}$$

$\pounds(f_m)$ results from the low frequency noise perturbing the imaginary part of the oscillator's inverted transfer function as already expressed by (7).

B. Experimental Procedure for Determining Noise Upconversion

As shown in the Appendix, D is a complicated expression involving device and resonator parameters. As a consequence, $K'_{\rm FM}$ is cumbersome to determine analytically. In this work $K'_{\rm FM}$ is determined experimentally. To do so consider a phase modulated signal, $s(t)$

$$s(t) = A\cos\left[\omega_0 t + \theta_0 + \frac{K'_{\rm FM} A_m}{f_m}\sin(\omega_m t)\right] \tag{13}$$

where A is the signal amplitude, ω_0 is the carrier frequency, A_m is the amplitude of the modulating signal, and ω_m is the modulating frequency; $K'_{\rm FM}$ is also referred to as the conversion efficiency of the modulating signal. The upconversion coefficient is now given by

$$K'_{\rm FM} = \frac{\gamma f_m}{A_m} \tag{14}$$

where γ is the modulation index. The equivalence of (10) and (14) can be shown by calculating the sideband power to carrier power ratio, $\pounds(f_m)$, for (13) for $\gamma \leq 0.2$ which gives

$$\pounds(f_m) \approx \frac{K'^2_{\rm FM} A^2_m}{4 f^2_m}. \tag{15}$$

Letting $A^2_m/2 = \overline{\Delta\epsilon^2(f_m)}$ and equating (15) and (9) will give (10). To determine $K'_{\rm FM}$, f_m or A_m is varied until the carrier is suppressed. This evaluation is based on the equation for the modulated signal, $s(t)$, which can be expressed in terms of Bessel functions as [25]

$$\begin{aligned} s(t) = A\{&J_0(\gamma)\cos\omega_0 t \\ &+ J_1(\gamma)[\cos(\omega_0+\omega_m)t - \cos(\omega_0-\omega_m)t] \\ &+ J_2(\gamma)[\cos(\omega_0+2\omega_m)t + \cos(\omega_0-2\omega_m)t]\cdots\} \end{aligned} \tag{16}$$

where $J_n(\gamma)$ is the nth order Bessel function. Using the fact that the carrier is suppressed (i.e. $J_0(\gamma)$ =0) for $\beta \approx 2.4$, $K'_{\rm FM}$ can then be calculated from (14). In this work, $K'_{\rm FM}$ was determined by superimposing a low frequency voltage on the base and varying the amplitude until the carrier was suppressed.

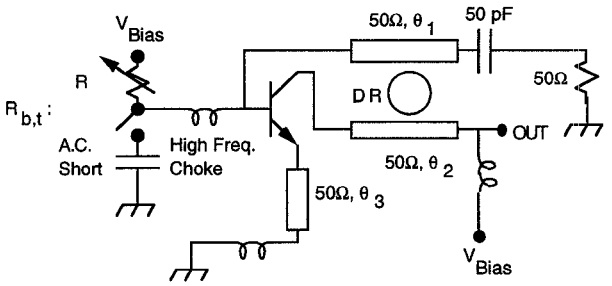

Fig. 1. Schematic diagram of the Dielectric Resonator Oscillator used in this Work.

III. HBT and Oscillator Description

The HBT used in these experiments is a *Npn* GaAs/AlGaAs device. It has five emitter fingers 2 μm × 20 μm giving a total emitter area of 200 μm^2. The devices were fabricated from MOCVD grown material using a self-aligned process which served to minimize parasitic resistances [4]. Their f_T and $f_{\rm max}$ are 20 and 40 GHz, respectively. The oscillator studied in this work is a Dielectric Resonator Oscillator (DRO). Parallel feedback is used with the dielectric resonator providing the necessary inductive feedback between the collector and the base [4]. Series feedback in the emitter circuit is used to improve output matching. A schematic diagram of the DRO is shown in Fig. 1. The collector and base bias are supplied from a single variable DC voltage source which is connected to the circuit through high frequency chokes. The base current is controlled via a 10-KΩ wirewound potentiometer (external to the fixture). The low frequency base termination $R_{b,t}$ can be switched from R (the value set by the wirewound potentiometer) to approximately 0 Ω (the impedance of the shunt capacitor). The high frequency choke allows signal transmission below 100 kHz.

Fig. 2 shows the measured spectrum for the low frequency short circuit base termination case, with $V_{\rm CE}$ = 5 V and I_C = 50 mA. The oscillation frequency is 11.02 GHz, and the output power was 5.6 dBm. This was verified to be the correct operating mode. No tuning of the emitter stub was attempted to maximize the output power. The output spectrum is clean. Beyond 2 kHz, the spectrum analyzer noise floor dominates the output. The external Q, $Q_{\rm ext}$, of the oscillator was measured using the frequency pulling technique described by Kurokawa [22], $Q_{\rm ext}$ ranges from approximately 1200 to 2200 as I_C is decreased from 50 mA to 20 mA.

IV. Phase Noise and AM Noise Results

The $\pounds(f_m)$ of the DRO was measured from 10 to 100 kHz using an HP3048A phase noise measurement system. Both the bias conditions and the low frequency base termination, $R_{b,t}$, were varied. $V_{\rm CE}$ was set to either 3 or 5 V, and I_C was varied from the minimum required to sustain oscillation to 50 mA. $R_{b,t}$ was set to either the bias resistance, R, needed for a given I_C, or 0 Ω (a.c. short) using a shunt capacitor (external to the test fixture) from the base to ground. The $R_{b,t}$ was not cooled because its room temperature noise voltage spectral density was calculated to be approximately two orders of magnitude below that measured for the HBT. Fig. 3 is a plot of $\pounds(f_m)$

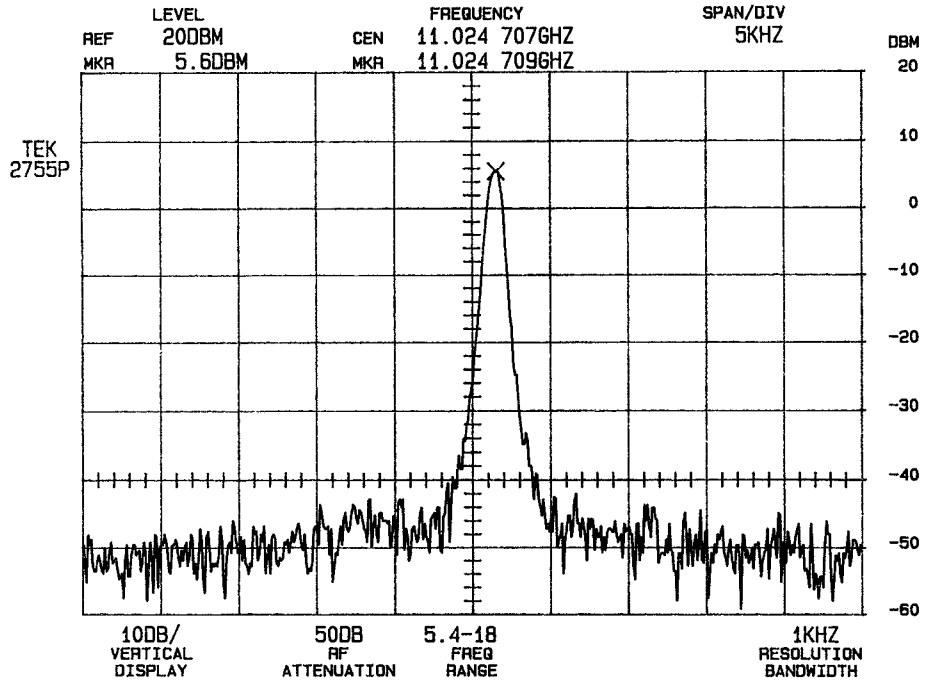

Fig. 2. Measured spectrum of the DRO for $V_{\rm CE} = 5$ V, $I_C = 50$ mA,and low frequency short circuit base termination.

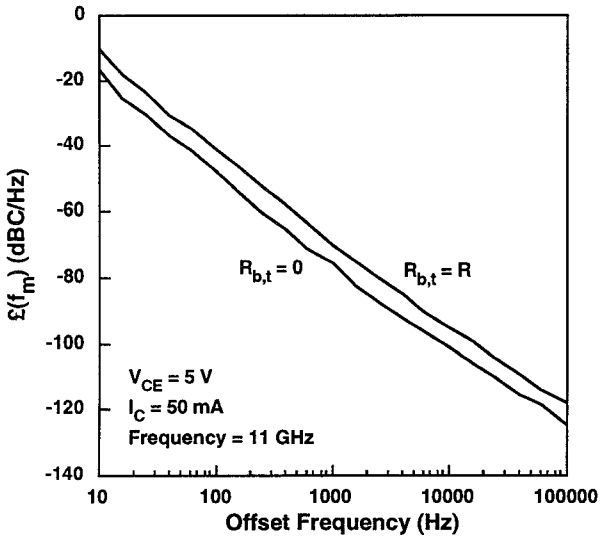

Fig. 3. Comparison of the phase noise, $\pounds(f_m)$, for $V_{\rm CE} = 5$ V and $I_C = 50$ mA for different base terminations.

versus frequency for $V_{\rm CE} = 5$ V, $I_C = 50$ mA, and two different base termination conditions. This figure clearly shows the impact of the base termination on $\pounds(f_m)$. The noise was reduced by about 4–7 dB over the entire measurement band when the base was a.c. short circuited at baseband frequencies.

The results for $\pounds(f_m)$ for various bias conditions and load terminations are summarized in Table I at a 10 kHz-offset. The best result, at a 10-kHz offset, is -101 dBc/Hz for $V_{\rm CE} = 5$ V, $I_C = 50$ mA, and $R_{b,t} = 0\ \Omega$. This decreased to -124 dBc/Hz, at a 100-kHz offset using the same bias conditions. $\pounds(10$ kHz) decreases as I_C is increased. For instance, $\pounds(10$ kHz) decreased from -94 dBc/Hz to -101 dBc/Hz as I_C was increased from 20 to 50 mA with $V_{\rm CE} = 5$ V and $R_{b,t} = 0$

TABLE I
$\pounds(10$ kHz) OF THE DRO FOR VARIOUS BIAS CONDITIONS AND BASE TERMINATIONS. $R_{b,t} = R$ IS THE CASE WHEN THE BASE IS TERMINATED INTO THE BIAS RESISTOR $R_{b,t} = 0$ IS THE CASE WHERE THE BASE IS TERMINATED INTO A SHUNT CAPACITOR

V_{CE} (V)	I_C (mA)	$\pounds$(10kHz)(dBc/Hz) $R_{b,t} = R$	$R_{b,t} = 0$
3	40	-91	-93
3	50	-93	-97
5	20	-91	-94
5	30	-89	-96
5	40	-92	-99
5	50	-95	-101

Ω. In addition, $\pounds(f_m)$ also decreases with the use of a short circuit base termination. The decrease varied from 2 to 7 dB depending on the bias condition. Moreover, $\pounds(f_m)$ decreased as $V_{\rm CE}$ is increased. For instance, for $I_C = 50$ mA and $R_{b,t} = 0\ \Omega$, $\pounds(f_m)$ decreased by about 4 dB as $V_{\rm CE}$ was increased from 3 to 5 V.

As discussed in Section II (7), one expects that the slope of $\pounds(f_m)$ versus frequency will follow an ideal $1/f^3$ relation when the phase noise is entirely due to upconversion of ideal $1/f$ noise. The $\pounds(f_m)$ for the oscillator reported here deviates from the $1/f^3$ dependence for off set frequencies greater than 400 Hz. Fig. 4 is a plot of the slope of $\pounds(f_m)$ as a function of frequency $(d\pounds\ (f_m)/df_m)$. Between 10 and 100 Hz the slope is about -30 dB/decade. However, this changes to about -23 dB/decade from 10 to 100 kHz. In general, at high frequencies, it was found that the slope varied between approximately -20 dB/decade and -25 dB/decade. This change in slope clearly shows that the measured $\pounds(f_m)$ is not simply due to upconversion of an ideal $1/f$ low frequency noise spectrum.

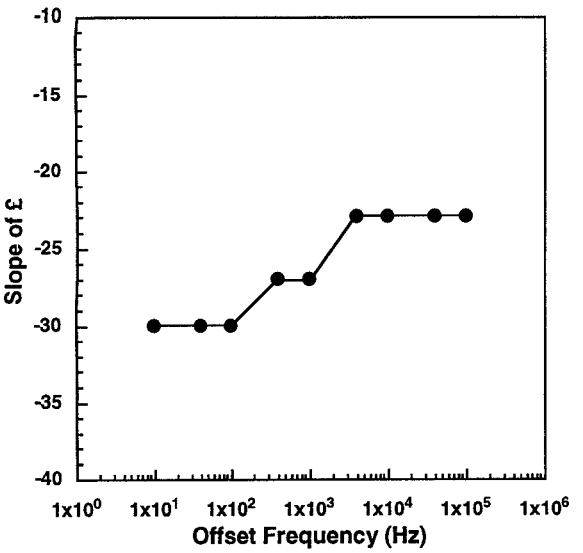

Fig. 4. Slope of oscillator phase noise, $\pounds(f_m)$, showing the deviation from −30 dB/decade.

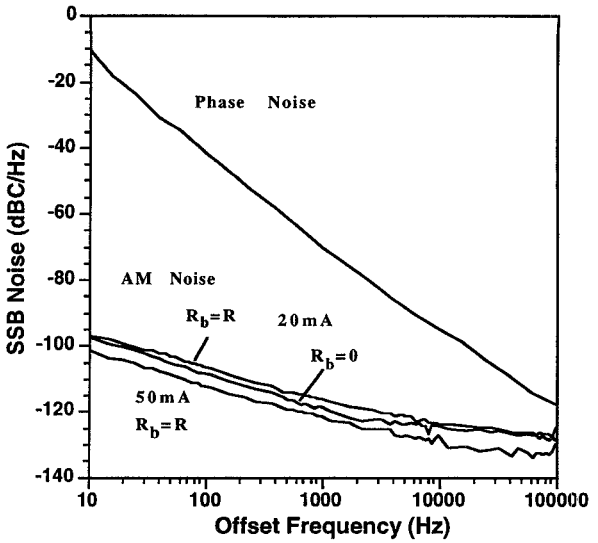

Fig. 5. Comparison of AM noise and $\pounds(f_m)$. The AM noise is shown for $I_C = 20$ mA with $R_{b,t} = 0$ and R, $I_C = 50$ mA with $R_{b,t} = R$. The $\pounds(f_m)$ curve corresponds to $I_C = 50$ mA with $R_{b,t} = R$.

Typically, one would expect that this change in the slope would be the result of the contribution due to additive noise. As will be seen later, this change might also be at least partially attributed to the HBT's low frequency noise spectra which is not entirely $1/f$ in nature, but can vary as a function of $1/f^{\alpha}$ with $0.4 \leq \alpha \leq 1.1$.

SSB-AM noise was measured by feeding the oscillator signal to a system consisting of a detector (Krytar Inc., 0.01–26.5 GHz) followed by a DC block and a preamplifier (North American Aerospace Corp., DC-100 kHz) and an HP3561A signal analyzer. The system noise floor was measured with the oscillator off. This was subtracted from the results measured when the oscillator was on. The difference was assumed to be due to the AM noise of just the oscillator itself. Fig. 5 is a plot of AM noise compared to phase noise. The AM noise is significantly lower than $\pounds(f_m)$ over the 10 Hz to 100 kHz measurement band. This low AM noise level is not surprising since the oscillator operates in a saturated amplitude mode. As a result, the amplitude noise is expected to be quite low. Since the $\pounds(f_m)$ is clearly the most dominant noise component, this paper concentrates on it and does not deal with the AM noise. In order to begin to understand the $\pounds(f_m)$ results, both the baseband noise of the HBT, and the upconversion coefficient, K'_{FM}, of the oscillator have been characterized and are discussed next.

V. Measurement of K'_{FM}

K'_{FM} was measured for this oscillator as a function of bias and frequency. The results are shown in Fig. 6. Measurements of K'_{FM} at 5 and 50 kHz showed that it was frequency independent. Similar results have been obtained for measurements made on MESFET's and HEMT's [12]. The bias dependent results showed that K'_{FM} decreases from 9.2 to 3.2 MHz/V with increasing I_C (20 to 50 mA, $V_{\mathrm{CE}} = 5$ V). The trend of reduced K'_{FM} with increased I_C is consistent with the $\pounds(f_m)$ trend with I_C described by the results in Table I. As will be shown in Section VI an increased I_C can sometimes result in increased baseband noise for the HBT. Thus the reduced oscillator noise at higher I_C will be primarily attributed to reduced upconversion in the oscillator. Measurements of Q indicate that it decreases with increasing I_C (see Section III). Recalling (12) this would cause K'_{FM} to increase with I_C. The $\frac{\partial V}{\partial \epsilon}$ term represents sensitivity to bias fluctuations. Since following the results of Fig. 6, K'_{FM} decreases with increasing bias, $\frac{\partial V}{\partial \epsilon}$ must be responsible for the decrease by also decreasing. Hence, the upconversion coefficient is reduced due to reduction in sensitivity to bias fluctuations. Although one expects the current and voltage to grow to some self-limiting condition when the device is oscillating, regardless of bias, this does not translate to insensitivity of noise to bias conditions. As stated already, $\frac{\partial V}{\partial \epsilon}$, and thus the sensitivity of upconversion and noise to bias fluctuations is indeed dependent on the bias. K'_{FM} showed less sensitivity to V_{CE}, changing from 3.2 to 2.2 MHz/V while varying V_{CE} from 5 to 3 V. To the authors' knowledge this resembles the behavior of MESFET oscillators where there is a very small variation with drain-source voltage.

It is interesting to compare the values of K'_{FM} obtained in this work with those measured for FET based oscillators. In the paper by Rhodin *et al.* [11], K'_{FM} ranged from 47 to 85 MHz/V when microstrip elements were used. K'_{FM} was reduced to about 1 MHz/V when dielectric resonator stabilization was used. This reflects the low-Q characteristics of the microstrip components. In [10] and [31] various DRO configurations were used with K'_{FM} ranging from 0.6 to 3 MHz/V. Free running oscillators had K'_{FM} of 140 MHz/V in the same work.

The $|\frac{\partial V}{\partial \epsilon}|$ term of K'_{FM} arises because the equivalent circuit parameters of the HBT are bias dependent and their perturbation, caused by the bias fluctuations, result in the upconversion of the baseband noise. To study the sensitivity of V to the HBT's equivalent circuit parameters, D was derived in terms of the oscillator's equivalent circuit parameters. The equivalent circuit analyzed is shown in Fig. 7 and the equivalent circuit values, which satisfy the oscillation conditions at 10 GHz, are

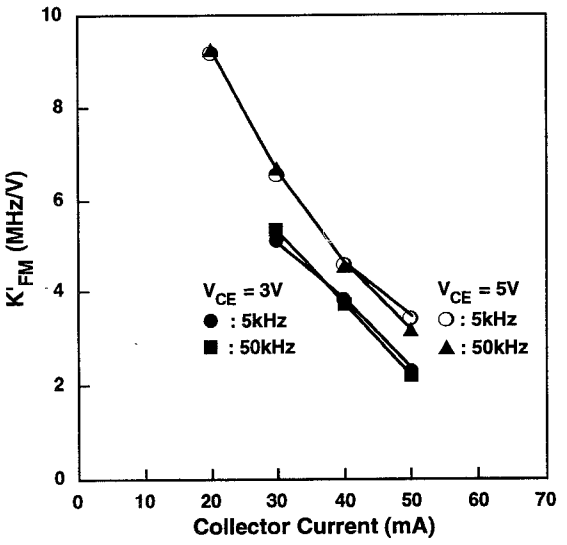

Fig. 6. The upconversion coefficient, K'_{FM}, as a function of bias and frequency.

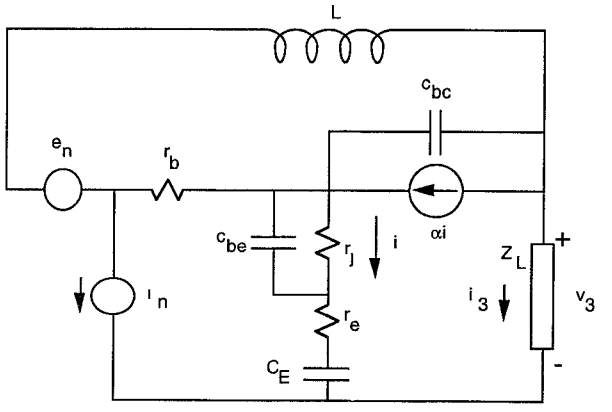

Fig. 7. Equivalent circuit used for calculating the inverted transfer function. The equivalent circuit is based on the Dielectric Resonator Oscillator shown in Fig. 1. Two additive noise sources are included. α is given by $\alpha = \alpha_0 \frac{e^{-j\omega\tau}}{1+j\frac{\omega}{\omega_0}}$.

in Table II. The additive noise is represented by the general case of a series noise voltage source, e_n, and a shunt noise current source, i_n. The presence of the two sources necessitates two different expressions for D. To simplify the present analysis we have ignored the correlation between the sources. D_{i_n} is the inverted transfer function derived for the noise current source. D_{e_n} is the inverted transfer function derived for the noise voltage source. The expressions for D_{i_n} and D_{e_n} are given in the Appendix. In order to determine the sensitivity of V (the imaginary part of D) to the equivalent circuit parameters, D_{i_n} and D_{e_n} were numerically differentiated with respect to each of the nonlinear circuit elements. For example, the numerical derivative of D_{e_n} with respect to c_{bc} was evaluated using

$$\frac{\Delta D_{e_n}}{\Delta c_{bc}} = \frac{D_{e_n 0} - D_{e_n 1}}{c_{bc} - c'_{bc}} \tag{17}$$

where c'_{bc} is c_{bc} reduced by one percent. $D_{e_n 0}$ is the value of the transfer function for the value of the parameters in Table II, $D_{e_n 1}$ is the value of the transfer function when

TABLE II
VALUES OF THE EQUIVALENT CIRCUIT PARAMETERS USED IN THE CALCULATIONS OF THE INVERTED TRANSFER FUNCTIONS

Circuit Element	Value
$r_b(\Omega)$	6.5
$r_j(\Omega)$	0.5
$c_{be}(pF)$	0.8
$c_{bc}(pF)$	0.141
α_0	0.945
$\omega_0(rad/sec)$	1.26×10^{11}
$\tau(psec)$	2.0
$C_E(pF)$	0.175
$L(nH)$	1.2
$Z_L(\Omega)$	84.03-j0.854

TABLE III
SENSITIVITY OF THE IMAGINARY PART OF THE INVERTED TRANSFER FUNCTIONS, D_{e_n} AND D_{i_n}, TO THE BIAS DEPENDENT EQUIVALENT CIRCUIT PARAMETERS AT 10GHz. r_j, c_{be}, c_{bc}, AND α_0 WERE CONSIDERED. THE GREATEST SENSITIVITY OCCURS FOR c_{bc}

	$\frac{\Delta V}{\Delta \alpha_0}$	$\frac{\Delta V}{\Delta r_j}(\Omega^{-1})$	$\frac{\Delta V}{\Delta c_{be}}(F^{-1})$	$\frac{\Delta V}{\Delta c_{bc}}(F^{-1})$
D_{in}	-2.7×10^{-1}	3.6×10^{-3}	2.8×10^{7}	-5.8×10^{12}
D_{en}	6.3×10^{-1}	-5.3×10^{-3}	6.2×10^{7}	-5.5×10^{12}

c_{bc} is replaced by c'_{bc}. The imaginary parts of the derivatives will indicate how sensitive V is to the circuit elements. The nonlinear elements that were considered are: r_j, c_{be}, c_{bc}, and α_0. Table III summarizes the results at 10 GHz. The greatest sensitivity is to the device capacitances c_{bc} and c_{be} where values of approximately $10^{12}/F$ and $10^{7}/F$, respectively, were obtained. The smallest sensitivity is for r_j which is approximately $10^{-3}/\Omega$.

VI. HBT Low Frequency Noise Characteristics

HBT low frequency noise, or baseband noise, can have many origins including: recombination, diffusion, trap, burst, and partition. Moreover, the physical location within the device can vary as well [26]. The work done on the low frequency noise characteristics of HBT's is quite limited in comparison to that done for Si BJT's. Early work dealt with double heterojunction bipolar transistors (DHBT's). The results of this work identified the presence of both $1/f$ noise and burst noise in the device. The corner frequencies were beyond 100 kHz. The work by [26] dealt with both the short circuit base and collector noise and found that the noise characteristics of these two ports were different. The work by [27] dealt with the excess white noise found in their HBT's. The excess noise turned out to be a single spectral component described by

$$S(\omega) = \frac{\tau}{1+(\omega\tau)^2} \tag{18}$$

where ω is the radian frequency, and τ is the time constant of the noise mechanism. Such a component is referred to as a Lorentz component. Tutt *et al.* [28], [29], dealt with

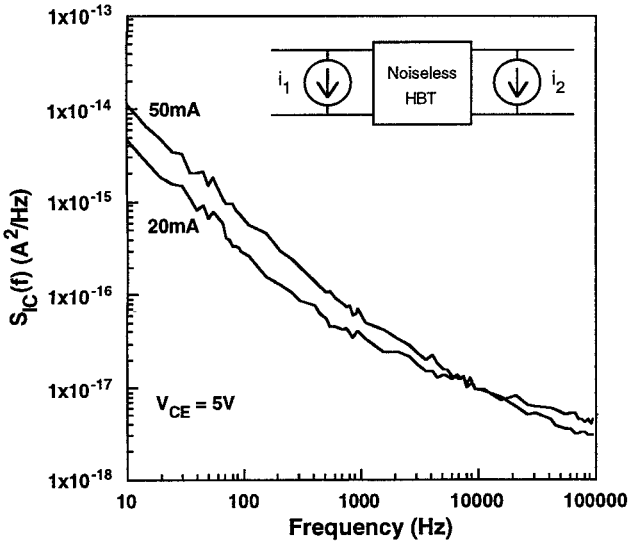

Fig. 8. Low frequency short circuit collector noise spectra, $S_{I_C}(f)$ as a function of bias and frequency for the HBT used in the oscillator. The inset contains the noise equivalent circuit used for HBT noise characterization.

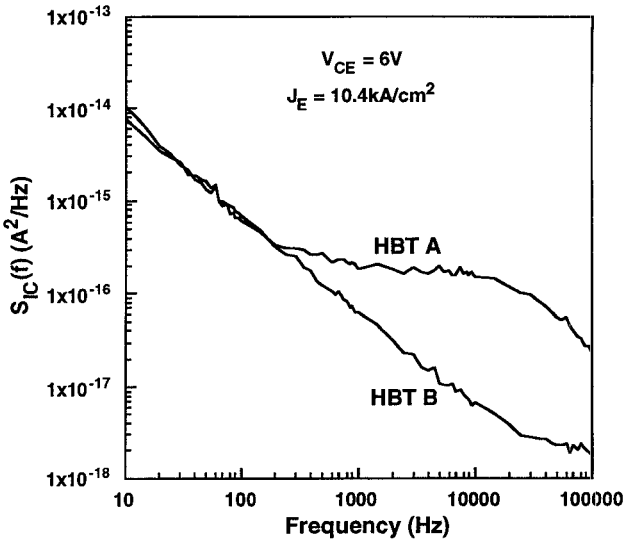

Fig. 9. Comparison of the low frequency noise spectra of two HBT's differing only in their layer design.

power HBT structures and observed recombination effects and significant Lorentz components. The Lorentz components were due to traps with an E_a of about 0.16 and 0.58 eV. The results also indicated saturation effects in the measured $1/f$ noise. Costa *et al.* [30], investigated bias and temperature dependences, surface passivation effects, the influence of the AlGaAs layer composition, and geometry effects.

Measurement of the noise spectra as a function of bias, frequency, and provides information about the origin(s) of the noise. The inset of Fig. 8 shows the noise equivalent circuit representation that is used. This model is used because the analysis of bipolar transistor noise is done in terms of noise currents. Referring to the inset, i_1 is the short circuit base noise current, with the collector terminal simultaneously short circuited. Its spectra is designated by $S_{I_B}(f)$ (A^2/Hz). i_2 is the short circuit collector noise current, with the base terminal simultaneously short circuited. Its spectra is designated by $S_{I_C}(f)$ (A^2/Hz). Even though one might expect a great deal of similarity between Si BJT's and GaAs/AlGaAs HBT's there is evidence that their noise mechanisms can be different. For instance, $S_{I_B}(f) = S_{I_C}(f)$ for Si BJT's [10] while $S_{I_B}(f) < S_{I_C}(f)$ for AlGaAs/GaAs HBT's [28].

Fig. 8 is a plot of $S_{I_C}(f)$ for $V_{CE} = 5$ V and $I_C = 20$ and 50 mA for the device used in the oscillator when it is in a nonoscillating mode. The measurements covered the 10 Hz to 100 kHz frequency range. The noise increased with I_C in the region which is approximately $1/f$ in nature ($S_{I_C}(f)$ increased 3.8 dB at 10 Hz) but, it decreased in the region where the spectra begin to flatten out ($S_{I_C}(f)$ decreased 1.7 dB at 100 kHz). The bias dependence of the $1/f$ noise spectra has been determined by measuring $S_{I_C}(f)$ for various I_C, and it is found to follow $S_{I_C}(10\text{ Hz}) \propto I_C^{1.7}$. This bias dependence suggests that recombination noise contributes to $S_{I_C}(10$ Hz). In general, the dependence of $S_{I_C}(f)$ on V_{CE} is weak.

The frequency dependence of $S_{I_C}(f)$ is clearly not $1/f$ over the entire measurement band. *Npn* GaAs/AlGaAs HBT's often do not display perfect $1/f$ noise spectra. It is known that a substantial noise bulge is seen in the $1/f$ noise spectra [28] in the vicinity of 10 kHz due to trapping. This is often associated with the n-type doping of the AlGaAs in the emitter and was present in the spectrum of the transistor tested here. As shown in Fig. 8, from 10 to 100 Hz the noise is essentially $1/f$ in nature. At higher frequencies this tends to reduce dra mAtically. For example, at frequencies greater than 10 kHz, it decreases to $1/f^{0.4}$ at $I_C = 20$ mA, or $1/f^{0.5}$ at $I_C = 50$ mA. This is likely due to traps which introduce a Lorentz component to the spectrum. This component will change the frequency dependence of the low frequency noise.

The actual spectral shape can vary widely among *Npn* GaAs/AlGaAs HBT's as shown in Fig. 9. This figure shows the spectra for two HBT's fabricated with the same process and having identical geometry, but different layer designs. One device clearly demonstrates a Lorentz component between 300 Hz and 100 kHz, while the other does not. The Lorentz component is large enough to cause the spectrum to essentially flatten out (i.e. $1/f^0$) from 1 to 10 kHz. Considering that nonlinear effects are present in the operation of an oscillator, these results indicate that the choice of HBT can impact the phase noise performance.

Up to this point, measurement of the collector noise spectra has assumed that the base was AC short circuited. For the general case where the base can have any termination, we denote the collector noise current spectra by $S'_{I_C}(f)$. To determine the impact of the base termination on the measured collector noise, $S'_{I_C}(f)$ was measured for the base termination used in the oscillator. Fig. 10 shows the measured low frequency noise spectra for the oscillator bias condition $V_{CE} = 5$ V and $I_C = 50$ mA. A clear increase of the $S'_{I_C}(f)$ for the nonzero $R_{b,t}$ case is shown. At 10 Hz the noise increased by 7.1 dB, while at 100 kHz it increased by 12.4 dB. This effect is easily understood by recalling the noise equivalent circuit of the HBT in Fig. 8. For the short circuit base condition, i_1 has no effect on the total output noise current, i_{out}. So $\overline{i_{\text{out}}^2} = \overline{i_2^2}$. This is due to i_1 being shunted out of the device. However, when the base termination is nonzero, some fraction, k, of i_1 flows into the

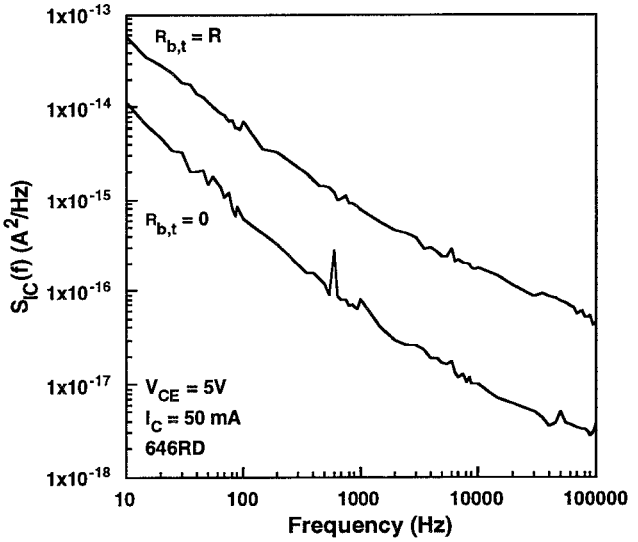

Fig. 10. Impact of the low frequency base termination on the output noise spectra.

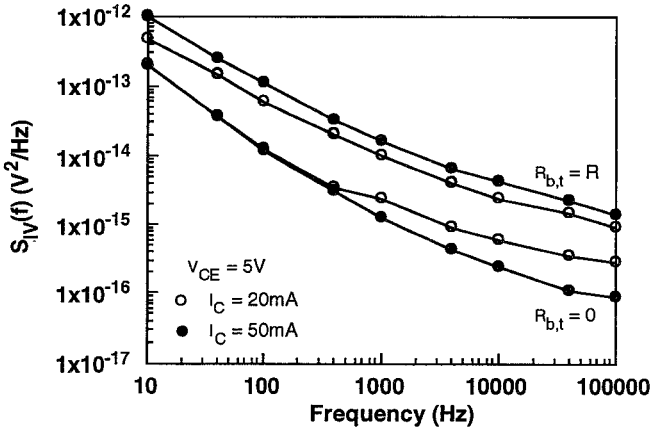

Fig. 11. Equivalent input noise voltage spectra for the HBT used in the DRO. The measured spectra correspond to $I_C = 20$ and 50 mA with the base terminated into R Ω and 0 Ω.

base where it is then amplified, by h_{fe}, and contributes to the total output noise current. Since i_1 and i_2 may be correlated, i_{out} becomes

$$\overline{i_{\text{out}}^2} = \overline{(kh_{fe}i_1 + i_2)^2} = (kh_{fe})^2\overline{i_1^2} + \overline{i_2^2} + 2ckh_{fe}\sqrt{\overline{i_1^2}\cdot\overline{i_2^2}} \tag{19}$$

where $c = \frac{\overline{i_1 i_2}}{\sqrt{\overline{i_1^2}\,\overline{i_2^2}}}$ is the correlation coefficient. The resulting amplitude of the output noise is affected by the correlation, input termination, magnitude of the input noise spectra, and gain of the device. For devices used in this work, a resistive base termination resulted in an increased noise at the output. In all of the measurements carried out, the corner frequency was never found to be below 100 kHz. This is consistent with the results of Costa [30].

The HBT baseband noise has been presented in terms of noise current spectral density, however, in the previous section the upconversion coefficient is given in units of MHz/V. In order to use the measured baseband noise it must be transformed into an equivalent input noise voltage spectral density, $S_{\text{IV}}(f)$ (V^2/Hz). The equivalent input noise voltage is obtained using

$$S_{\text{IV}}(f) = \frac{S_{I_C}(f)R_L^2}{A_V^2(f)} = \frac{S_{I_C}(f)}{g_m^2(f)} \tag{20}$$

where R_L is the collector load resistor used for the baseband noise measurement and $A_V(f)$ is the voltage gain of the HBT in the test circuit. Fig. 11 is a plot of $S_{\text{IV}}(f)$ for the HBT measured for $I_C = 20$ mA and 50 mA with the base terminated into either R Ω or approximately 0 Ω. For the case where the base is terminated into 0 Ω the $S_{\text{IV}}(f)$ spectra are equal at low frequencies. As the frequency increases the noise at 50 mA is less than that at 20 mA. In fact, the S_{IV} (100 kHz), for the 50 mA case, is almost 5 dB less. This occurs because the voltage gain is greater for the 50 mA case (A_v (100 kHz) = 6.1) compared to the 20 mA case (A_v (100 kHz = 4.0) and, as shown in Fig. 8, the S_{I_C} (100 kHz) is approximately 1.7 dB lower for the 50-mA case. For the case where the base is terminated into R Ω the $S_{\text{IV}}(f)$ is approximately 2 dB greater for the 50-mA case over the entire frequency range. This is due to the fact that the base noise current of the HBT increases with bias [29] which, through (19) and (11), results in an effectively larger $S_{\text{IV}}(f)$.

It is useful to compare the $S_{\text{IV}}(f)$ of HBT's and MESFET's, however, the appropriate normalization must be used. $S_{\text{IV}}(f)$ of MESFET's is normalized to the gate width according to Graffeuil [10]. The MESFET's used in the work by Camiade *et al.* [31] had S_{IV}(10 kHz) ranging from 3.33 × 10^{-18}V^2/Hz/μm to 133 × 10^{-18} V^2/Hz/μm. The correct normalization for the HBT noise depends on the origin of the noise. Test structures were not available to determine if S_{I_C} was either periphery or area dependent, consequently, it was normalized to the emitter width. Since g_m is also proportional to the emitter width, S_{IV} is inversely propotional to the emitter width through (20). The HBT here had S_{IV}(10 kHz)= 2.4 × 10^{-18} V^2/Hz/μm for the best $\pounds(f_m)$ case ($I_C = 50$ mA and $R_{b,t} = 0$). This is comparable to the lowest values of the MESFET's.

VII. Calculation of $\pounds(f_m)$ Using K'_{FM} and Device Baseband Noise

Using the experimentally determined values of K'_{FM} and $S_{\text{IV}}(f)$, the phase noise, due to upconversion of baseband noise, can be calculated using 10 log[$\pounds(f_m)$] of (15). $A_m^2/2$ is replaced by the equivalent input noise voltage spectral density, $S_{\text{IV}}(f)$, of the HBT. This assumes that the device noise, measured in an nonoscillating condition, is valid for the oscillating condition. Fig. 12(a) and (b) contain measured and calculated $\pounds(f_m)$ for $V_{\text{CE}} = 5$ V and $I_C = 20$ mA for $R_{b,t} = 0$ Ω and R. The agreement in both cases is very good, typically less than 3-dB difference. This shows that the $\pounds(f_m)$ can be described by the upconversion of the device's baseband noise.

Measured and calculated $\pounds(f_m)$ were also compared for the cases of $V_{\text{CE}} = 5$ V and $I_C = 50$ mA with $R_{b,t} = 0$ Ω and R [Fig. 13(a) and (b)]. In the case of $R_{b,t} = R$ the agreement is again very good showing that $\pounds(f_m)$ can be described by

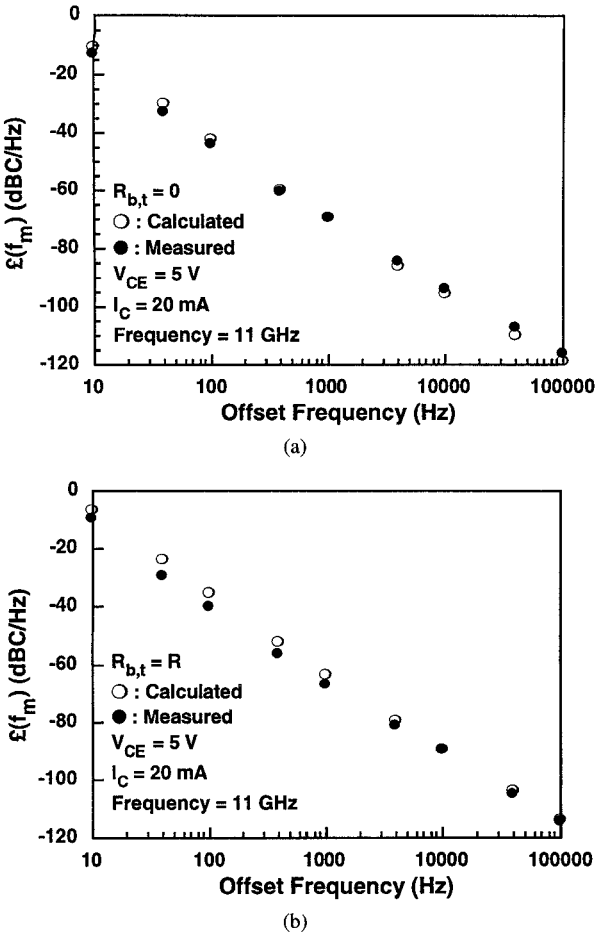

Fig. 12. Comparison of calculated and measured $\pounds(f_m)$ for $V_{\rm CE} = 5$ V and $I_C = 20$ mA. These results are for $R_{b,t} = 0$ and R base terminations.

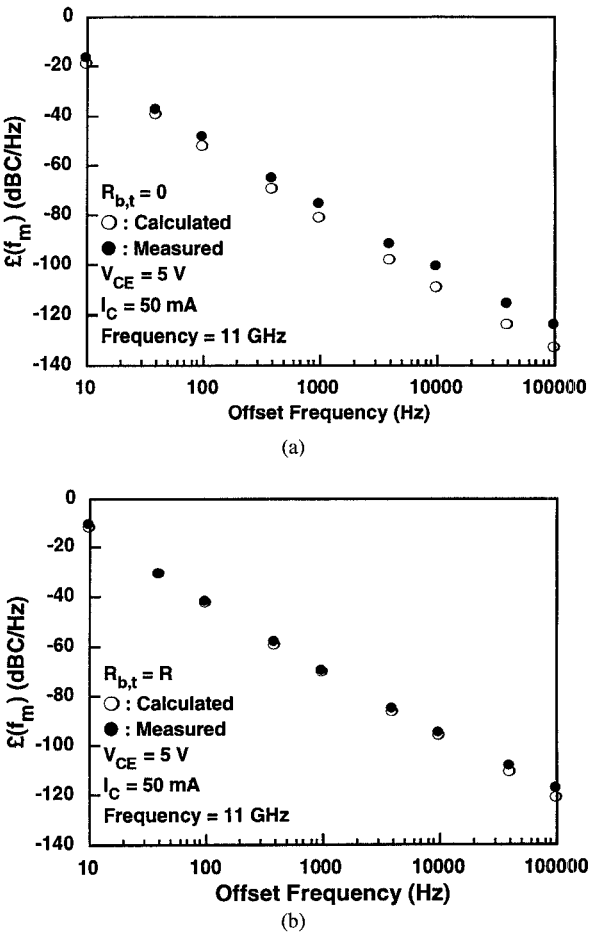

Fig. 13. Comparison of calculated and measured $\pounds(f_m)$ for $V_{\rm CE} = 5$ V and $I_C = 50$ mA. These results are for $R_{b,t} = 0$ and R base terminations.

the upconversion of the device's baseband noise. In contrast, for the case of $R_{b,t} = 0\ \Omega$, the agreement is good at very low offset frequencies, however, an increasing discrepency occurs at higher frequencies. The discrepancy is as great as 9 dB at 100 kHz. This indicates, for this case, $\pounds(f_m)$ is not simply due to upconverted baseband noise. Recalling (2), the complete oscillator noise description requires the modulation conversion matrix. There are three sources of phase noise: 1) additive noise at the operating frequency, 2) upconverted baseband noise and 3) AM-PM conversion. In the case of $R_{b,t} = 0$, the upconverted baseband noise is not dominant and one, or both, of the other two sources dominates. In the $R_{b,t} = R$ case, the equivalent input noise voltage, $S_{\rm IV}(f)$, is larger. Since the oscillator is operating in a saturated amplitude mode this will not affect the AM-PM contribution. Moreover, the additive noise contribution is not affected either. Agreement of theory and experiment is therefore better since the only significant noise mechanism present is baseband noise upconversion; (11) used for the theoretical prediction accounts only for noise upconversion and consequently predict better the oscillator perfor mance in such cases.

Comparing the trends observed for $K'_{\rm FM}$ (Fig. 6) and for $S_{\rm IV}(f)$ (Fig. 11) with those of $\pounds(f_m)$, the increase in $\pounds(f_m)$ with $R_{b,t} = R$ is entirely due to the increased $S_{\rm IV}(f)$. The bias dependence of $\pounds(f_m)$, however, cannot be explained in terms of the bias dependence of $S_{\rm IV}(f)$. For instance, increasing I_C from 20 to 50 mA, with $R_{b,t} = R$, results in a 2.4-dB increase in $S_{\rm IV}$ (10 kHz) , while $\pounds$(10 kHz) decreases approximately 4 dB. The bias dependence of $\pounds$(10 kHz) is therefore dominated by that of $K'_{\rm FM}$ which decreases with increasing I_C. On the other hand, the frequency dependence of $\pounds(f_m)$ is determined by the baseband noise and not $K'_{\rm FM}$ which was shown to be frequency independent.

VIII. Conclusion

The $\pounds(f_m)$ and AM noise of a HBT DRO have been measured as a function of bias and low frequency base termination. The SSB-AM noise is far less than $\pounds(f_m)$. Best $\pounds(f_m)$ obtained was -124 dBc/Hz at a 100 kHz offset at $V_{\rm CE} = 5$ V, $I_C = 50$ mA, and a short circuit base termination. $\pounds(f_m)$ decreased by as much as 7 dB (at a 10-kHz offset frequency) by increasing I_C, from 20 to 50 mA. In addition, $\pounds(f_m)$ also decreased by as much as 7 dB (at a 10-kHz offset frequency) through the use of a short circuit low frequency base termination due to shunting the base noise of the transistor. The roles of the upconversion coefficient, $K'_{\rm FM}$, and the HBT's baseband noise in $\pounds(f_m)$ were studied. $K'_{\rm FM}$ decreases with increasing I_C which is consistent with $\pounds(f_m)$. On the otherhand, the baseband noise tended to increase slightly with increasing I_C. In most cases measured $\pounds(f_m)$ could be modeled usng the HBT's baseband noise and, $K'_{\rm FM}$, with agreement typically within 3 dB. Under some conditions either cross-modulation or additive noise may

$$D_{i_n} = \frac{i_n}{v_3 Y_L} \tag{21}$$

$$= \frac{[Y_2(\alpha Y_E - Y_2) + (Y_L + Y_1 + Y_2)(g_b + Y_2 + Y_E(1-\alpha))](g_b + Y_1)}{Y_L[Y_1(g_b + Y_2 + Y_E(1-\alpha)) - g_b[\alpha Y_E - Y_2]]} - \frac{[Y_1 Y_2 + g_b(Y_L + Y_1 + Y_2)]g_b}{Y_L[Y_1(g_b + Y_2 + Y_E(1-\alpha)) - g_b[\alpha Y_E - Y_2]]} - \frac{Y_1}{Y_L} \tag{22}$$

become more significant. Modeling $\pounds(f_m)$ using K'_{FM} and the baseband noise shows that the frequency dependence of $\pounds(f_m)$ is governed by the frequency dependence of the baseband noise since K'_{FM} is frequency independent.

APPENDIX
TRANSFER FUNCTION FOR THE DRO

The oscillator used in this study was a dielectric resonator oscillator with feedback between the collector and the base (Fig. 1). The small signal equivalent circuit of the oscillator is shown in Fig. 7. The additive noise sources, e_n and i_n are included as well. Since there are two additive noise sources there are two transfer functions D_{i_n} and D_{e_n} for i_n and e_n, respectively. Equations (21) and (22) are shown at the top of this page, where

$$Y_1 = \frac{1}{j\omega L}$$
$$Y_2 = j\omega C_{bc}$$
$$Y_E = \left[r_E + \frac{r_j}{1 + j\omega C_{be} r_j} + \frac{1}{j\omega C_E}\right]^{-1}$$
$$g_b = \frac{1}{r_b}$$
$$Y_L = \frac{1}{Z_L}. \tag{23}$$

Y_L is the total load admittance, and v_3 is the voltage across Y_L. In this analysis the effect of the DRO is approxi mated by a lumped element inductor, L.

$$D_{e_n} = \frac{e_n}{i_3 Z_L} \tag{24}$$

$$= -\left[\frac{Z_2(1-\alpha)(r_b + Z_1) + (Z_E + Z_L)(r_b + Z_1 + Z_2)}{Z_2 Z_L}\right] \tag{25}$$

where

$$Z_1 = j\omega L$$
$$Z_2 = \frac{1}{j\omega C_{bc}}$$
$$Z_E = \left[r_E + \frac{r_j}{1 + j\omega C_{be} r_j} + \frac{1}{j\omega C_E}\right]. \tag{26}$$

ACKNOWLEDGMENT

The authors would like to thank F. Goodman for the assembly of the DRO. The authors also thank North American Aerospace for donating the preamplifier used in the low frequency noise measurements, and the AM noise measurements.

REFERENCES

[1] B. Bayraktaroglu *et al.*, "5 Watt monolithic HBT amplifier for broadband X-band applications," in *IEEE Microwave and Millimeter-Wave Monolithic Circ., Symp. Dig.*, pp. 43–46, May 1990.
[2] M. E. Kim, "12–40 GHz low harmonic distortion and phase noise performance of GaAs heterojunction bipolar transistors," in *IEEE GaAs IC Symp. Dig.*, 1988, pp. 117–120.
[3] M. A. Khatibzadeh *et al.*, "High power and high efficiency HBT VCO circuit," *IEEE GaAs IC Symp. Dig.*, 1989, pp. 11–14.
[4] M. A. Khatibzadeh and B. Bayraktaroglu, "Low phase noise heterojunction bipolar transistor oscillator," *Electron. Lett.*, vol. 26, no. 16, pp. 1246–1247, Aug. 1990.
[5] C. C. Leung *et al.*, "A 0.5 μm silicon bipolar transistor for low phase noise oscillator applications up to 20 GHz," in *Proc. 1985 IEEE MTT-S*, pp. 383–386.
[6] M. Purnell, "The dielectric resonator oscillator—A new class of microwave signal source," *Microwave J.*, pp. 103–108, Sept. 1981.
[7] Avantek Oscillator Catalog.
[8] Y. Kwon, D. Pavlidis, T. Brock and D. C. Streit, "A D-band monolithic fundamental oscillator using InP-based HEMT's," in *Proc. IEEE 1993 Microwave and Millimeter-Wave Monolithic Circuits Symp.*, pp. 49–52
[9] O. Ishihar *et al.*, "A highly stabilized GaAs FET oscillator using a dielectric resonator feedback circuit in 9–14 GHz," *IEEE Trans Microwave Theory Tech.*, vol. 28, no. 8, pp. 817–824, Aug. 1980.
[10] J. Graffeuil *et al.*, "Ultra low noise GaAs MESFET microwave oscillators," *Noise in Phys. Syst. and 1/f Noise*, pp. 329–332, 1983.
[11] H. Rhodin, C. Su and C. Stolte, "A study of the relation between device low-frequency noise and oscillator phase noise for GaAs MESFET's," in *Proc. 1984 IEEE MTT-S*, pp. 267–269.
[12] M. Pouysegur, J. Graffeuil, J. Seautereau and J. Fortea, "Comparative study of phase noise in HEMT and MESFET microwave oscillators," in *Proc. 1987 IEEE MTT-S*, pp. 557–559.
[13] K. K. Agarwal *et al.*, "Dielectric resonator oscillators using GaAs/AlGaAs heterojunction bipolar transistors," in *Proc. 1986 IEEE MTT-S*, pp. 95–98.
[14] N. Hayama *et al.*, "A low noise Ku-band AlGaAs/GaAs HBT oscillator," in *Proc. 1988 IEEE MTT-S*, pp. 679–682.
[15] M. Madihian *et al.*, "A 20–28 GHz AlGaAs/GaAs HBT monolithic oscillator," *IEEE GaAs IC Symp. Dig.*, 1988, pp. 113–116.
[16] M. Madihian *et al.*, "A low noise microwave oscillator employing a self-aligned AlGaAs/GaAs HBT," *IEEE Trans Microwave Theory Tech.*, vol. MTT-37, no. 11, pp. 1811–1814, Nov. 1989.
[17] A. Adar and R. Ramachandran, "An HBT MMIC wideband VCO," in *Proc. 1991 IEEE MTT-S*, pp. 247–250.
[18] D. B. Leeson, "A simple model of feedback oscillator noise spectrum," *IEEE Trans Microwave Theory Tech.*, MTT-vol. 33, no. 3, pp. 233–242, Mar. 1985.
[19] B. T. Debney and J. S. Joshi, "A theory of noise in GaAs FET microwave oscillators and its experimental verification," *IEEE Trans ED*. vol. 30. no. 7, pp. 769–776, Sept. 1983.
[20] H. J. Siweris and B. Schiek, "Analysis of noise upconversion in microwave FET oscillators," *IEEE Trans Microwave Theory Tech.*, MTT-vol. 33, no. 3, pp. 233–242, Mar. 1985.
[21] R. Pucel and R. Ramachandran, "Near carrier noise in fet oscillators," in *Proc. 1983 IEEE MTT-S*, pp. 282–284.
[22] K. Kurokawa, "Injection locking of microwave solid state oscillators," *Proc. IEEE*, vol. 61, no. 10, pp. 1386–1410, Oct. 1973.
[23] A. Riddle, "Oscillator noise: Theory and characterization," Ph.D. thesis, N.C. State University, 1986
[24] A. Riddle and R. Trew, "A new approach to low phase noise oscillator design," in *Proc. IEEE/Cornell Conf. Advanced Concepts in High Speed Semiconductor Devices and Circ.*, July, 1985, pp. 302–311.
[25] F. G. Stremler, *Introduction to Communication Systems*. Reading, MA:

Addison-Wesley, ch. 6, 1977.
[26] X. Zhang, A. Van der Ziel, K. Duh and H. Morkoc, "Burst and low-frequency generation and recombination noise in double-heterojunction bipolar transistors," *IEEE ED*, vol. EDL-5, no. 7, pp. 277–279, July 1984.
[27] G. Blasquez, C. Limaskul, J. P. Bailbe, A. Marty and C. Antarasana, "Current noise in GaAlAs/GaAs heterojunction bipolar transistors," *Noise in Phys. Syst. and 1/f Noise*, pp. 195–197, 1985.
[28] M. N. Tutt, D. Pavlidis and B. Bayraktaroglu, "An assessment of noise sources and characteristics of AlGaAs/GaAs heterojunction bipolar transistors," in *Proc. 16th Int. Symp. GaAs and Rel. Comp.*, 1989, pp. 701–706.
[29] M. Tutt, D. Pavlidis, A. Khatibzadeh and B. Bayraktaroglu, "Low frequency noise characteristics of self-aligned GaAs/AlGaAs heterojunction bipolar transistors," Submitted to *IEEE Trans. ED*.
[30] D. Costa and J. Harris, "Low frequency noise properties of N-p-n AlGaAs/GaAs heterojunction bipolar transistors," *IEEE Trans ED*, vol. 39, no. 10, pp. 2383–2394, Oct. 1992.
[31] M. Camiade et al., "Low noise design of dielectric FET oscillators," in *Proc. 13th Euro. Microwave Conf.*, 1983.

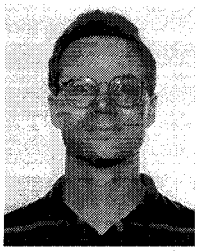

Marcel N. Tutt received the Ph.D. in electrical engineering from the University of Michigan, Ann Arbor, MI in 1994. He received the B.A.Sc. (1980) and M.A.Sc. (1983) in electrical engineering from the University of Waterloo, Ontario, Canada. The Ph.D. research primarily dealt with the low frequency and the high frequency noise properties of heterojunction transistors. The Master's thesis dealt with the analysis of microstripline structures using the method of Moments. Prior to pursuing the Ph.D.

He worked in the Military Avionics Division and the Systems Research Center of Honeywell where he was involved in the design, analysis, and characterization of GaAs monolithic microwave integrated circuits. While at the University of Michigan he developed noise characterization capability from baseband to 18 GHz and small signal characterization up to 100 GHz. His presentations and publications are in the areas of low frequency and high frequency noise of heterojunction transitions, noise measurement techniques, InP HEMT stability, and InP HEMT MMIC's. His current research interests include characterization and analysis of new device technologies for circuit and system applications.

Dimitris Pavlidis (S'73–M'76–SM'83–F'93) received the B.Sc. degree in physics from the University of Patras, Patras, Greece, in 1972, and the Ph.D. degree from the University of Newcastle, Newcastle-upon-Tyne, UK, in 1976. He continued as postdoctoral fellow at Newcastle until 1978, where he studied microwave semiconductor devices and circuits.

In 1978 he joined the High Frequency Institute of the Technical University of Darmstadt, Germany, where he worked in III-V devices and establishing a new semiconductor technology facility. In 1980 he worked at the Central Electronic Engineering Research Institute, Pilani, India, as UNESCO consultant. During 1980–1985 he was an engineer and manager of a GaAs Monolithic Microwave Integrated Circuits (MMIC) Group of Thomson-CSF, Corbeville, France. He was responsible for projects on monolithic power and broadband amplifiers, tunable oscillators, optical preamplifiers, phase shifters, attenuators, their technology and process evaluation, and the establishment of a component library for MMIC applications. He holds six patents on MMIC applications and has written on microwave semiconductor devices and circuits. His current research interests include design and fabrication of HEMT's HBT's MOCVD growth of InP-based and GaN materials, and monolithic heterostructure integrated circuits.

Dr. Pavlidis was awarded the European Microwave Prize for his work on InP based monolithic integrated HEMT amplifiers. In 1991 he received the decoration of "Palmes Acdèmiques" in the order of Chevalier by the French Ministry of National Education for his work in education. In 1992, he received the Japan Society of Promotion of Science Fellowship for Senior Scientists/Professors from the Japanese Government, and the Humboldt Research Award for Distinguished Senior US Scientists.

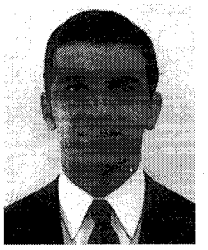

Ali Khatibzadeh received the Ph.D. degree in electrical engineering from North Carolina State University in 1987.

Subsequently, he joined the GaAs Microwave Branch of Texas Instruments (TI) Central Research Laboratories where he was involved in the development of microwave & millimeterwave GaAs devices and ICs. From 1992–1994, he was manager of the GaAs Microwave HBT Branch. Presently, he is manager of the RF Design Branch of TI's Semiconductor Group.

Burhan Bayraktaroglu (M'78-SM'93) received the B.Sc and Ph.D. degrees in 1974 and 1978, respectively, both in electrical engineering, from the University of Newcastle Upon Tyne, England.

He was at the Air Force Avionics Laboratory as a visiting scientist from 1978 to 1981, working on the development of GaAs surface passivation techniques. From 1981 to 1992, he was at Texas Instruments Central Research Laboratories, Dallas, involved in the development of advanced GaAs microwave devices and circuits. As a member of Technical Staff, he was responsible for the development of monolithic IMPATT circuits and heterojunction bipolar transistors (HBTs). He was manager of GaAs HBT Microwave branch from 1989 to 1992, coordinating research in the development of HBT devices and IC's. From 1992 to 1994, he was with North Carolina State University, College of Engineering, Raleigh, involved in on-site research in high power microwave HBTs and applications at the Wright Laboratory of Air Force at the Wright-Patterson AFB, OH. He is now an advisory engineer at the Advanced Technology Laboratory of Westinghouse Electric Corporation in Baltimore, MD, involved in the development of high efficiency HBT MMIC amplifiers.